Observation of water vapor in the stratosphere of Jupiter with the Odin Space Telescope.

T. Cavalié, F. Billebaud, N. Biver, M. Dobrijevic, E. Lellouch, J. Brillet, J. Lecacheux, A. Hjalmarson, A. Sandqvist, U. Frisk, et al.

Observation of water vapor in the stratosphere of Jupiter with the Odin Space Telescope

T. Cavalié [a,*] , F. Billebaud [a], N. Biver [b], M. Dobrijevic [a], E. Lellouch [b], J. Brillet [a], A. Lecacheux [b], Å. Hjalmarson [c], Aa. Sandqvist [d], U. Frisk [e], M. Olberg [c], The Odin Team, E.A. Bergin [f]

[a] *Université Bordeaux 1; CNRS; OASU; LAB, UMR 5804, 331270 Floirac, France*

[b] *LESIA, Observatoire de Paris, 92195 Meudon, France*

[c] *Onsala Space Observatory, 43992 Onsala, Sweden*

[d] *Stockholm Observatory, 10691 Stockholm, Sweden*

[e] *Swedish Space Corporation, 17104 Solna, Sweden*

[f] *Harvard-Smithsonian Center for Astrophysics, Cambridge MA 02138, USA*

Abstract

The water vapor line at 557 GHz has been observed with the Odin space telescope with a high signal-to-noise ratio and a high spectral resolution on November 8, 2002. The analysis of this observation as well as a re-analysis of previously published observations obtained with the Submillimeter Wavelength Astronomy Satellite seem to favor a cometary origin (Shoemaker-Levy 9) for water in the stratosphere of Jupiter, in agreement with the ISO observation results. Our model predicts that the water line should become fainter and broader from 2007. The observation of such a temporal variablity would be contradictory with an IDP steady flux, thus supporting the SL9 source hypothesis.

Key words: Jupiter, atmosphere, water, spectroscopy, Odin space telescope

1 Introduction

The Infrared Space Observatory has detected water vapor in the stratospheres of the giant planets (Feuchtgruber et al. 1997; Feuchtgruber et al. 1999; Lellouch 1999). The large amount of water measured above the condensation level of vapor (cold trap at the tropopause) implies the presence of an external source of oxygenated compounds (Moses et al. 2000b; Lellouch et al. 2002). These compounds could be brought by interplanetary dust particles (IDP), sputtering from the rings and/or satellites and large cometary impacts. Observations of Jupiter carried out by ISO tend to prove that most of the stratospheric water is due to the Shoemaker-Levy 9 (SL9) comet impacts in July 1994 (Lellouch et al. 2002), whereas Bergin et al. (2000) obtained satisfactory fits to the Submillimeter Wavelength Astronomy Satellite (SWAS) data by considering IDP infall, with a constant flux of 2.0×10^{6} $cm^{-2}.s^{-1}$.

The submillimeter satellite Odin was launched in 2001 and obtained a high resolution spectrum of Jupiter's water vapor line (1_{10}-1_{01}) at 557 GHz on November 8, 2002. This spectrum is presented in this work as well as a reanalysis of SWAS observations. Spectral analysis combined with the use of our photochemical model (Ollivier et al. 2000, adapted to Jupiter) provides new clues which help understanding the origin of water vapor in the stratosphere

* Tel: +33-5-5777-6123; fax: +33-5-5777-6110
Email address: Thibault.Cavalie@obs.u-bordeaux1.fr (T. Cavalié).

of Jupiter.

A description of the observations is given in Sect. 2. Our photochemical and radiative transfer models are described in Sect. 3. Our results are presented in Sect. 4 and the different sources of H_2O are discussed in Sect. 5.

2 Observations

The space telescopes SWAS and Odin observed the water vapor 557 GHz line on Jupiter in 1999, 2001 (SWAS) and 2002 (Odin). The resulting brightness temperature spectra have a signal-to-noise ratios of ∼17, 10 and 16 respectively for the 1999, 2001 and 2002 observations. The spectral resolution is about 1 km.s^{-1} for the SWAS spectra and 0.6 km.s^{-1} for the Odin spectrum.

The SWAS spectra are corrected for the Double Side Band (DSB) response of the instrument. Nevertheless, the SWAS spectra show broad features at 100 km.s^{-1} and more, which cannot be reproduced in models. These wings, probably due to instrumental effects as mentionned in Bergin et al. (2000) and Lellouch et al. (2002), cause an uncertainty on the continuum level of the emission. More details on the SWAS 1999 and 2001 observations can be found in Bergin et al. (2000) and Lellouch et al. (2002).

The Odin observations were carried out with the Acousto-Optical Spectrometer (AOS) in a classical position switching mode (Olberg et al. 2003). The receivers are operated in a Single Side Band (SSB) mode. The spectral band is 1 GHz. As Jupiter has a strong continuum emission at this frequency, stationary waves are generated within the instrument, causing ripples on the spectrum (Fig. 1). The subtraction of the ripples is the source of an uncertainty of 10%

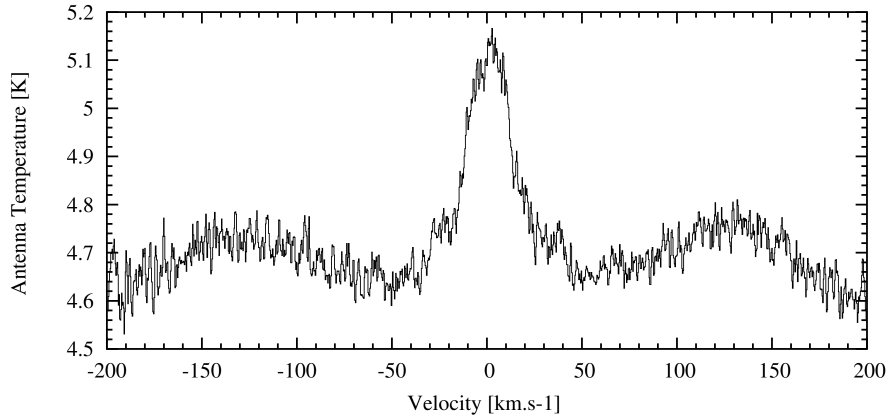

Fig. 1. Odin observations of Jupiter at the H_2O (1_{10}-1_{01}) line frequency on November 8, 2002. The observed antenna temperature is displayed as a function of velocity. The signal-to-noise ratio is 16.

on the line contrast and some uncertainty on the line wing shape.

As the beam size (3.3'×4.5' for SWAS and 2.1' for Odin) is larger than the planet size (∼35-40"), all the observed features correspond to the emission of the whole planet. The line width is dominated by the smearing effect because of limb equatorial velocity ∼12.6 km.s^{-1} of the planet (Bergin et al. 2000). As no absolute calibration has been done for the Odin observations, all results are discussed in terms of line-to-continuum ratios and the Odin/SWAS observed continuum have been rescaled to the brightness temperature scale of our model (T_B=128.6 K).

3 Modeling

We describe, in this section, details of our data analysis procedure that can be summarized in the following way:

- A water vertical profile is simulated from a time-dependent 1D photochemical model. The main parameters that affect this profile are the altitude and the magnitude of water deposition (in the case of a sporadic cometary origin), the magnitude of the water influx (in case of a steady interplanetary dust particle flux) and the eddy diffusion coefficient in the stratosphere.

- A radiative-transfer model computes a synthetic spectrum for each water vapor profile.
- Comparison of observational data and synthetic spectra enables to constrain parameters of the photochemical model.

3.1 Photochemical modeling

We used a time-dependent photochemical model, derived from the model developed for Saturn by Ollivier et al. (2000) and which has been adapted to the case of the atmosphere of Jupiter. For each altitude and each chemical compound i, the code solves the continuity equation

$$\frac{\mathrm{d}n_i}{\mathrm{d}t} = P_i - n_i L_i - \mathrm{div}\,(\phi_i) \tag{1}$$

where n is the concentration, P the chemical production, L the chemical loss and ϕ the vertical flux. This is a one-dimensional model since only the vertical transport is considered.

The model includes 46 oxygenated compounds and hydrocarbons and 593 reactions (photolysis processes and chemical reactions). Condensation near the tropopause is also considered. The eddy diffusion coefficient profile we took comes from Moses et al. (2005). We chose their nominal eddy profile called "model C"(see Sect. 5). The influx rates of oxygenated compounds (proportion of H_2O, CO_2 and CO) and H atoms were also taken from Moses et al. (2005).

Moses et al. (2000) showed that an IDP source is more likely than a ring/satellite source since there is a difference of ∼2 orders of magnitude in the estimated fluxes. This is the reason why we chose to compare the results of two models: an IDP source model and a low-IDP+SL9 source model. For the sake of simplicity, the latter model will be called the SL9 model hereafter. The lack of spatial resolution of the observations allowed us to use disk-averaged mixing ratio vertical profiles for water, even if the SL9 impacts were all located in the southern hemisphere. The only input parameter we had to fix to test the IDP source hypothesis is the external flux of infalling water $\Phi^{IDP}_{H_2O}$. In order to test the SL9 source hypothesis, we have built vertical profiles at the time of the impacts (July 1994) and let them evolve with the photochemical model until the time of the observations (September 1999, January 2001 for the SWAS data and November 2002 for the Odin data). The initial water vertical profiles have been built on the base of a low stationnary external flux and a sporadic input, due to the comet. The low stationnary input flux is modeled via an IDP model with a flux $\Phi^{IDP}_{H_2O}$=4×10^4 cm^{-2}.s^{-1} (Lellouch et al. 2002). This value is 2 orders of magnitude lower than a pure IDP model (see Sect. 4). The sporadic input of water due to the impacts was modeled via two parameters: the deposition pressure p_0 and the initial mixing ratio q_0 above the p_0 level (see Lellouch et al. 2002 for more details). For each computation, the value of q_0 was set to a constant value as a function of altitude (above the p_0 level).

Thus, we have two possibilities for the SL9 models. The first one consists of fixing the value of p_0 and adjusting the value of q_0 with the data. In the second case, we fix q_0 and adjust p_0. Some constraints exist on both p_0 and q_0. The most reliable constraint is probably the fact that the deposition level that was

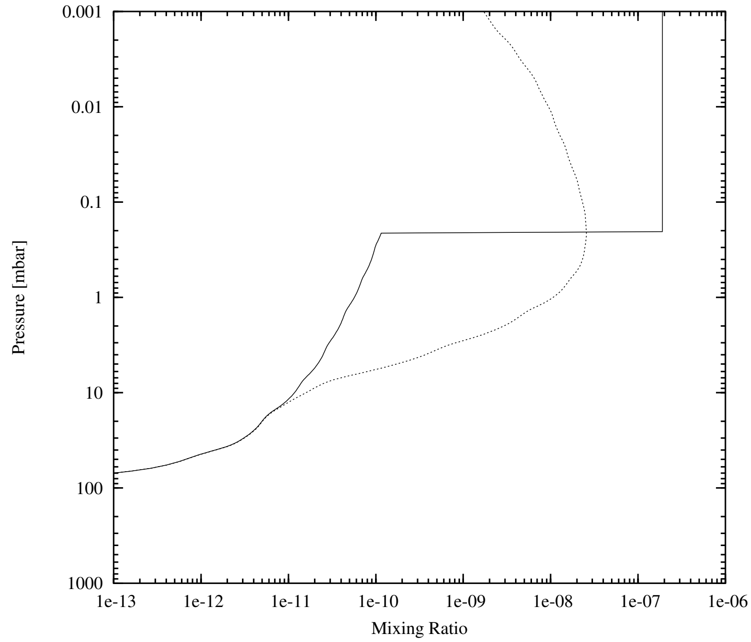

Fig. 2. Example of SL9 source vertical profiles of water at the time of the SL9 impacts (07/1994) in solid line and at the time of the Odin observations (11/2002) in dashed lines. The evolution of water abundance is computed by the photochemical model. The water vapor mixing ratio is displayed as a function of atmospheric pressure. Profiles correspond to a fixed value of p_0=0.2 mbar, and an adjusted value of q_0=1.9×10^{-7}.

observed for CO during the SL9 impacts is 0.2±0.1 mbar (Moreno 1998). From CO and CS post-impact observations, Lellouch et al. (1995), Lellouch et al. (1997) and Moreno et al. (2001) derived p_0 levels of 0.3 mbar, 0.04-0.2 mbar and 0.1 mbar (respectively). The other constraint lies on the observed column density of water vapor. Lellouch et al. (2002) inferred that the H_2O/CO ratio is equal to 0.07 in mass according to the entire ISO data set, thus fixing the H_2O column density to $(2.0\pm0.5)\times10^{15}$ cm^{-2}. Such a value lead to the derival of a mixing ratio of water vapor of 6×10^{-8} above the deposition level. An example of a SL9 model profile at the time of the impacts and at the time of the Odin observations is shown on Fig. 2.

3.2 Radiative transfer modeling

We modeled the observed submillimeter radiation with a line-by-line non-scattering radiative transfer model. We computed synthetic spectra of the H_2O 557 GHz line. The program represents the approximate spherical geometry of the planet so that planetary disk and limb contributions are taken into account. We assumed an uniform distribution of all other opacity sources and we adopted a mean thermal profile (see Fig. 3) of the atmosphere of Jupiter (Fouchet et al. 2000a) since our beam size is larger than the observed planetary disk. Continuum opacity is dominated by H_2-He-CH_4 collision-induced absorption (Borysow et al. 1985, 1986 and 1988). Following Moreno (1998), the opacity due to the far wings of ammonia and phosphine lines was also included. We used the Fouchet et al. (2000b) ammonia and phosphine mixing ratio vertical profiles (see Fig. 4). Spectroscopic parameters for NH_3, PH_3 and H_2O were taken from Pickett et al. (1998). The line widths are determined by the collisional line widths for H_2 and He broadening. The broadening γ and temperature dependance exponent n values that we took for NH_3, PH_3 and H_2O are summarized in Table 1. All lines, except the NH_3 ones, were assumed to be Voigt-shaped. Following Moreno (1998), we took a modified Van Vleck and Weisskopf line profile for ammonia.

The rapid rotation of Jupiter (9.9 h) induces the smearing of the disk-averaged line on the spectrum, because of the Doppler shifts due to the gas rotation velocity (12.6 km.s^{-1} at the eastern and western limbs). The way this effect is taken into account is described in Bergin et al. (2000).

We briefly come back to the use of disk-averaged vertical profiles of mixing

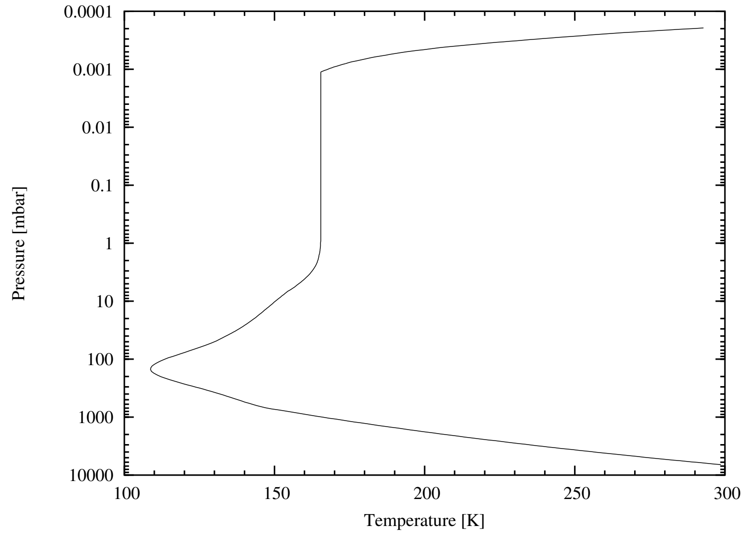

Fig. 3. Disk-averaged thermal profile of the atmosphere of Jupiter. The tropopause temperature is 109 K. The profile is isothermal (T=165.4 K) between 1 mbar and 10^{-3} mbar. Reference: Fouchet et al. (2000a).

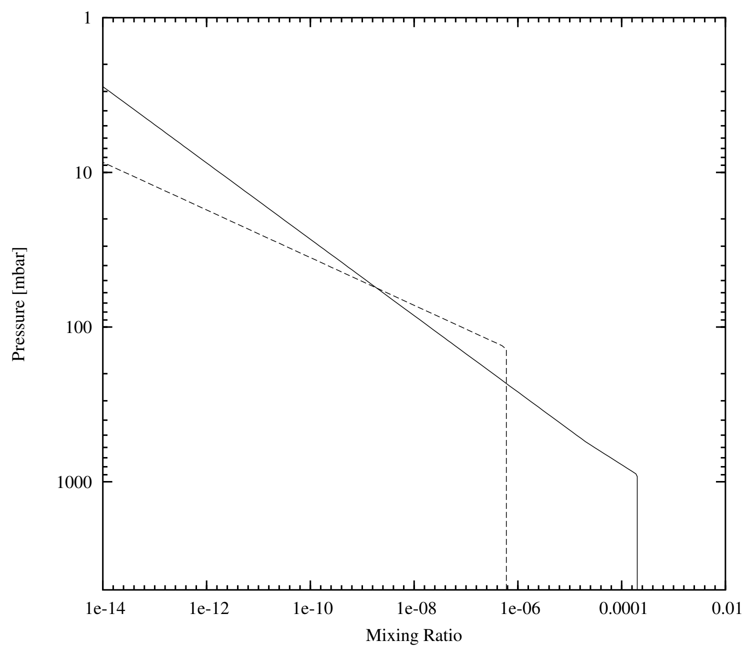

Fig. 4. Ammonia (solid line) and phosphine (long-dashed lines) mixing ratio vertical profiles as a function of pressure in Fouchet et al. (2000b).

ratio. The fact that the SL9 impacts were all located in the southern hemisphere is not a limitation to our hypothesis. All the impacts occured at the

γ	H_2	He	Jupiter
NH_3	0.069		0.069
PH_3 (2-1)	0.1064	0.0606	0.1001
H_2O	0.0811	0.0228	0.0731
n	H_2	He	Jupiter
NH_3	0.67		0.67
PH_3	0.73	0.30	0.67
H_2O	0.9	0.50	0.85

Table 1

Collisional line width γ $\left[cm^{-1}.atm^{-1}\right]$ (at 300 K) and temperature dependance factor n for NH_3, PH_3 and H_2O with H_2 and He and for Jupiter (a blank space means that no data are available). References: Berge & Gulkis (1976) and Brown & Peterson (1994) for NH_3, Levy et al. (1993,1994) for PH_3 and Dutta et al. (1993) for H_2O.

latitude of 44°S. Longitudinal mixing proved to be efficient in the submillibar region. Indeed, HCN was observed at such pressure levels a few months after the comet impacts and the maps showed that it had already spread over several degrees in longitude (Bézard et al. 1997). So, the deposits quickly formed a longitudinal belt after the impacts. Thus we have to take into account the background amount of water present in the stratosphere of Jupiter, which is due to the low IDP flux ($\Phi^{\rm IDP}_{\rm H_2O}$=4×10^4 cm^{-2}.s^{-1}), and the SL9 input located at 44°S, which is modeled via the parameters p_0 and q_0. By averaging those two kinds of vertical profiles over the surface of the planet, we obtain the kind of profile shown in Fig. 2 (see "hybrid model" in Lellouch et al. 2002), where p_0 is determined by the SL9 input and where q_0 is multiplied by the ratio between the surface of the SL9 longitudinal belt and the total surface of the planet. Using this approach, the values of q_0 we derive from the observations are disk-averaged values. A disk-averaged water vertical profile is adapted since the beam size is greater than the planet size.

4 Results

The best-fit models have been determined with a χ^2 minimization process. All profiles and column density values are disk-averaged. One must note that an uncertainty of 5 K on the thermal profile would add an uncertainty of 0.4×10^{15} cm^{-2} on the water vapor column density, 0.3×10^{-7} on q_0 (in the case of a SL9 origin) and 0.6×10^6 cm^{-2}.s^{-1}(in the case of an IDP origin).

4.1 SWAS data

The observed Rayleigh-Jeans temperature continuum of the 1999 and 2001 observations are 126.4 K (Bergin et al. 2000) and 118.0 K (Lellouch et al. 2002) at -60 km.s^{-1} respectively. After rescaling the continuum value to the brightness temperature continuum of our model, it appears that only the SL9 models give satisfactory fits to both sets of data, either in the wings or in terms of line contrast. If we fit the line center, the IDP model with $\Phi^{\mathrm{IDP}}_{\mathrm{H_2O}}$=$(3.4\pm0.5)\times10^6$ cm^{-2}.s^{-1} results in spectra which have too broad wings (see Fig. 5). It is not possible fit within the 1-σ error bars the line center and the wings at the same time. The best-fit model for both SWAS datasets is obtained with a SL9 model with p_0=0.2 mbar and q_0=$(1.8\pm0.5)\times10^{-7}$ (see Figs. 5 and 6), leading to an

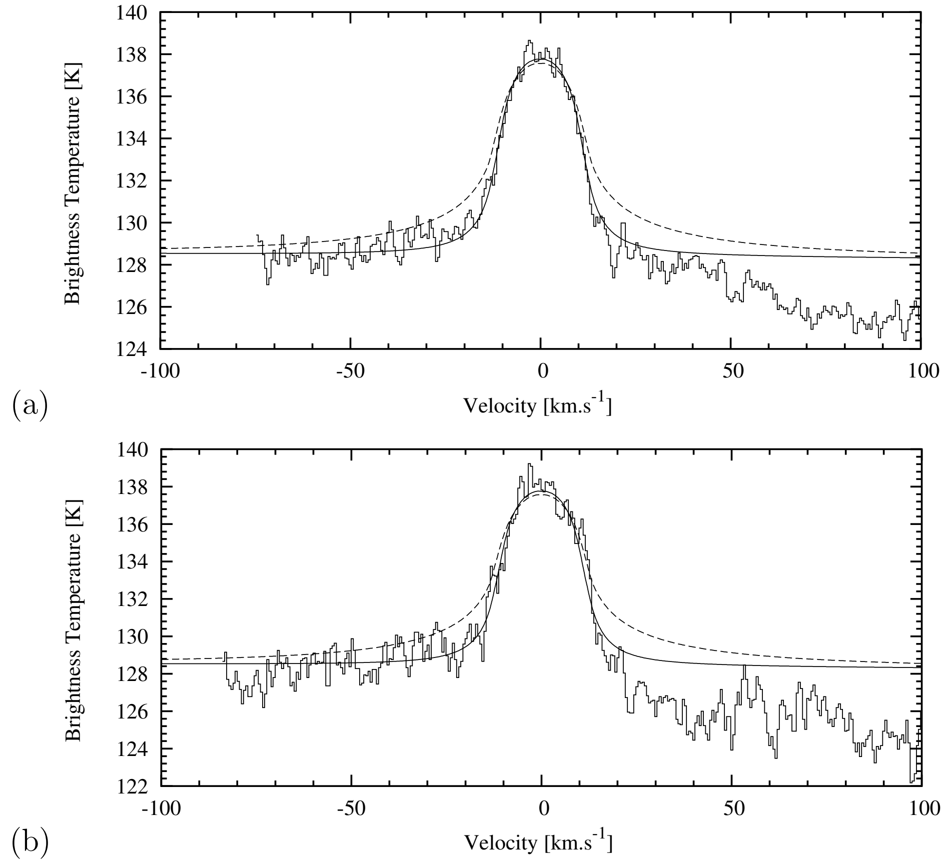

Fig. 5. Best-fit model to the (a) SWAS 1999 and (b) 2001 data obtained with a SL9 model with the initial parameters p_0=0.2 mbar and q_0=1.8×10^{-7} (solid lines). The IDP models (long-dashed lines) correspond to infall fluxes of $\Phi^{IDP}_{H_2O}$=3.4×10^6 cm^{-2}.s^{-1} for 1999 and 2001 respectively.

initial (in July 1994) column density of (3.5±1.0)×10^{15} cm^{-2}.

Nevertheless, the value of the continuum of both observations is quite uncertain, mostly due to the broad spectral features. Shifting downward the value of the continuum level within the error bar, it is possible to derive new values of the IDP flux that permits us to obtain synthetic spectra that match the SWAS data. For instance, if the continuumm of the 1999 and 2001 observations are set to 125.4 K and 117.0 K (respectively) instead of 126.4 K and 118 K (respectively) and then rescaled to the brightness temperature continuum

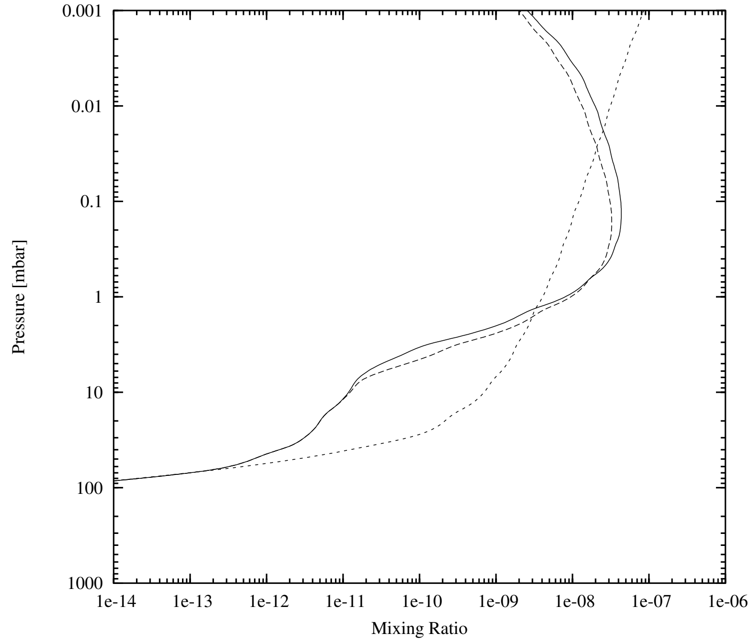

Fig. 6. Water mixing ratio vertical profiles as a function of pressure for a SL9 model with p_0=0.2 mbar and q_0=1.8×10^{-7} at the time of the SWAS 1999 observations (solid line) and at the time of the SWAS 2001 observations (long-dashed lines) and for IDP models with a steady flux of water $\Phi^{\rm IDP}_{\rm H_2O}$=3.4×$10^6$ cm^{-2}.s^{-1} (short-dashed line). The column density of water is $n_{\rm H_2O}$=3.5×10^{15} cm^{-2} for the SL9 model at the time of the impacts and $n_{\rm H_2O}$=2.6×10^{15} cm^{-2} for the IDP model.

of our model (T_B=128.6 K), then the fits of IDP models are far better (Fig. 7). The flux we derive is $\Phi^{\rm IDP}_{\rm H_2O}$=(3.7±0.5)×$10^6$ cm^{-2}.s^{-1} and the corresponding column density is (2.8±0.4)×10^{15} cm^{-2}. The synthetic spectrum is within the 1-σ error bars on the data over the [−80:+20] km.s^{-1} range. Finally, the IDP model cannot be ruled out at this stage, because of the uncertainty on the continuum level of each observation, even if a χ^2 analysis shows that the SL9 model gives a better match to the data than the IDP model. All the IDP models that are considered for the SWAS data in what follows are models with downward shifted continuum (to 125.4 K and 117.0 K, for 1999 and 2001 respectively).

The SL9 model where q_0 is fixed to 6×10^{-8} also gives a good fit for p_0=(0.45± 0.09) mbar (see Fig. 8). Here, the error bar on the p_0 value is not due to the 1-σ level of the spectrum. Indeed, the synthetic spectra with either p_0=0.37 mbar or p_0=0.54 mbar are outside the 1-σ level of the spectrum. This error bar is due to the fact that the integration step of the photochemical model is 5 km. This results in 0.09 mbar steps in the 0.2-0.6 mbar region. Taking p_0=0.45 mbar and q_0=6×10^{-8}, the column density of water is $(2.6\pm0.6)\times10^{15}$ cm^{-2} at the time of the impacts.

4.2 Odin data

After removing the ripple pattern, the line shows some asymmetry in the line wings. This, as well as the noise level, is a limitation in the determination of the best-fit model. Testing the IDP fluxes leads us to retrieve of a lower flux than the flux retrieved from the SWAS data. Indeed, the χ^2 minimum is obtained for a flux value of $\Phi^{\mathrm{IDP}}_{\mathrm{H_2O}}=(3.4\pm0.5)\times10^6$ cm^{-2}.s^{-1} (see Fig. 9). This result is compatible with the SWAS initial results (before shifting downward the Rayleigh-Jeans temperature continuum). If we try to fit the line with an averaged best-fit model to the SWAS/Odin data ($\Phi^{\mathrm{IDP}}_{\mathrm{H_2O}}=3.6\times10^6$ cm^{-2}.s^{-1}), then the line center is better reproduced (see Fig. 9). Nevertheless, such a modeling results in broader wings, but they still are within the 1-σ error bars.

As for the SL9 model, restraining the bulk of water above an initial pressure level of 0.2 mbar, results in narrower lines than the IDP model. The line center as well as the wings are well reproduced with the synthetic spectra. When fixing p_0 to 0.2 mbar, the optimum water mixing ratio above this level is $q_0=2.0\times10^{-7}$. The uncertainty is 0.5×10^{-7}. When fixing q_0 to 6.0×10^{-8}

(Lellouch et al. 2002), p_0 is found to be (0.54±0.09) mbar (see Fig. 10). The latter model implies a column density of $(3.2\pm0.6)\times10^{15}$ cm^{-2} at the time of the comet impacts.

5 Discussion

The best-fit model parameters for each observation, as derived from χ^2 minimization, are summarized in Table 2. From this set of parameters, we derived averaged values. For each model (IDP, SL9 with q_0 fixed and SL9 with p_0 fixed), the value obtained is affected a weight related to the signal-to-noise ratio of the observation. Doing this way, we obtained the averaged values used in Fig. 11.

First of all, when considering the SL9 source hypothesis and fixing the value of q_0 at 6×10^{-8}, we derive a deposition pressure level p_0 in the range of 0.45-0.54 mbar. The column density we derived is consistent with the value of Lellouch et al. (2002). However, even if our model does not provide a more precise value of p_0, the range of the values we derive is outside the ranges derived by Lellouch et al. (1997) and Moreno (1998) from CO observations at millimeter wavelengths at the time of the impacts, which are 0.04-0.2 mbar and 0.2±0.1 mbar (respectively). Therefore, we regard this possibility as unlikely with regard to both SWAS and Odin data.

So, the models we have to compare are the IDP model and the SL9 model with p_0=0.2 mbar. We derived an external flux of water, originating from an IDP source, of $\Phi^{IDP}_{H_2O}=(3.6\pm0.5)\times10^6$ cm^{-2}.s^{-1}. This value is greater than the one derived by Bergin et al. (2000) by a factor of less than 2. From their physical model, which only included vertical transport (no chemical or photochemical processes), the authors derived a deposition flux of 2.0×10^6 $cm^{-2}.s^{-1}$. To obtain a narrower line from their model and thus to obtain their best-fit model, they increased the mixing ratio over pressure slope ($-d(\log q)/d(\log p)$) of their physical profile from 0.8 to 1.3. Nevertheless, as noted by the authors, changing the slope could not simulate precisely the effects of photolysis, chemical reactions and the non-linearity of the interactions between these processes as well as vertical transport and condensation. Taking photolysis and chemical losses into account, they would probably have obtained a higher value for the flux consistent with our result.

With a SL9 model, we obtain $q_0=(1.9\pm0.5)\times10^{-7}$ when fixing $p_0=0.2$ mbar. Lellouch et al. (2002) derived a column density of $(2.0\pm0.5)\times10^{15}$ cm^{-2} at the time of the ISO observations. The column density we derived is $(3.7\pm1.0)\times10^{15}$ cm^{-2} at the time of the impacts. This value is greater than the ISO value, but by taking photolysis, chemical reactions, vertical transport and condensation, this value decreases down to $(3.1\pm0.8)\times10^{15}$ cm^{-2} at the time of ISO observations. This value is still above the Lellouch et al. (2002) value, but there is a small overlap on the ranges of values. Moreover, considering an uncertainty of 5 K on the thermal profile ends up in an additional uncertainty of 0.4×10^{15} cm^{-2} on the column abundance. So, these values could well be consistent and an intermediate value of column density should be compatible with all inferred values. As the water vapor vertical profile of Lellouch et al. (2002) was computed from a vertical transport model, the ISO data should be re-analysed with a more complete photochemical model. This work still has to be done and its results could be directly comparable to ours.

The SL9 model quoted above better reproduces the line contrast as well as the

SWAS 1999 and 2001			
Model	$\Phi^{IDP}_{H_2O}$[cm^{-2}.s^{-1}]	p_0 [mbar]	q_0
IDP	(3.7±0.5)×10^6	-	-
SL9 (q_0 fixed)	4.0×10^4	(0.45±0.09)	6×10^{-8}
SL9 (p_0 fixed)	4.0×10^4	0.2	(1.8±0.5)×10^{-7}
Odin 2002			
Model	$\Phi^{IDP}_{H_2O}$[cm^{-2}.s^{-1}]	p_0 [mbar]	q_0
IDP	(3.4±0.5)×10^6	-	-
SL9 (q_0 fixed)	4.0×10^4	(0.54±0.09)	6×10^{-8}
SL9 (p_0 fixed)	4.0×10^4	0.2	(2.0±0.5)×10^{-7}

Table 2

Best-fit model parameters for each set of data and each model, from which the averaged best-fit value are derived (see text).

line wings than the IDP model (see Fig. 11). A χ^2 analysis clearly indicates that the SL9 model gives better fits to the data. However, all the IDP synthetic spectra are within the 1-σ error bars on all observations. So, this model cannot be ruled out at this stage.

If the observed water would come from the SL9 comet, then the non-steady state created by the deposition of the cometary material above the p_0 level in our model should evolve towards a steady state where the only observable source of water would be the low IDP flux (4×10^4 cm^{-2}.s^{-1} in our model). From our computations, such a state is reached ∼400 years after the impacts. As a result, the downward diffusion of water as well as the photochemical/chemical losses effects would first desaturate the line. Thus, the line contrast should first increase with time (see Fig. 12). Our photochemical model predicts that the line center temperature of the line should increase by 0.76 K from 1999 to 2007. Taking the noise level of the SWAS 1999 observations into account, our model predicts that this effect could only be observed in 2007 by reaching a signal-to-noise ratio of 50 with the Odin telescope. Afterwards, the amount of water decreasing more and more with time at submillibar pressures, the line should become fainter and broader and should tend towards the line that would be due to the low IDP flux only (see Fig. 12). This change should be observable with Herschel-HIFI.

One must not forget that the shape of the water vertical profile computed with a photochemical model highly depends on the vertical eddy diffusion coefficient profile $K(z)$. Due to strong uncertainties in the chemical scheme, each photochemical model derives, from comparison with observational data, a new value of $K(z)$ that can differ by about one order of magnitude at some altitudes (see Dobrijevic & Parisot 1998, Dobrijevic et al. 2003 and Hébrard et al. 2007 for a detailed discussion on this point). For instance, as shown on Fig. 7 of Moses et al. (2005), many different $K(z)$ profiles have been inferred from past observations. At the submillibar pressure range, $K(z) \simeq 5 \times 10^4$ $cm^{-2}.s^{-1}$ within a factor of 2 (Moreno et al. 2003). According to the Moses et al. (2005) model C value used in this work, $K(z)$ is equal to 7.8×10^4 $cm^{-2}.s^{-1}$. At pressures between 0.1 mbar and 100 mbar (tropopause level), Gladstone et al. (1996) found values of $K(z)$ higher by a factor of $\sim$3. So we have to consider the fact that another choice in the $K(z)$ profile could change our results. In the lower stratosphere, our adopted $K(z)$ profile gives a lower limit to $K(z)$ values (see Fig. 7 in Moses et al. 2005). By taking the Gladstone et al.(1996) $K(z)$ profile, we would obtain an eddy mixing in the lower stratosphere more efficient than in our study and it would result in more water above the condensation level. The direct impact on the spectra of such a change in the $K(z)$ profile would be a broadening of the wings. Thus, the IDP origin synthetic spectra would be out of the 1-σ error bars of the SWAS and Odin observations. Finally, taking Moses et al. (2005) model C as a $K(z)$ profile is a conservative way of analysing the observed lines with regard to the implications noted above.

6 Conclusion

In this paper, we have shown that the high signal-to-noise ratio observations of water vapor in the stratosphere of Jupiter, carried out with SWAS and the Odin telescope between 1999 and 2002, favor a SL9 origin for water. Indeed, all observations are better fitted when the bulk of water is restricted to sub-millibar pressures. In our disk-averaged and simplified deposition model of the SL9 water, we derived a water mixing ratio of 1.9×10^{-7} above an initial pressure deposition level of 0.2 mbar. In this model, a low IDP flux of 4×10^{4} $cm^{-2}.s^{-1}$ was also taken into account. This suggests a localised input of water, in terms of altitude, which is contradictory with a steady state resulting from an IDP permanent flux. Nevertheless, all synthetic spectra obtained from an IDP flux of $\Phi^{IDP}_{H_2O}$=$(3.6\pm0.5)\times10^{6}$ $cm^{-2}.s^{-1}$ give fits that are within the 1-σ error bars of the observations, but the χ^2 value is greater than the one computed from the SL9 model. In view of these results, the ISO data of 1997 should be re-analysed using the model developped in this work.

Further observations, reaching a higher signal-to-noise ratio are needed to state on the origin of water vapor in the stratosphere of Jupiter, even if the SL9 origin is favored by both SWAS and Odin observations. The analysis of the latest Odin observations (August 2007) is underway. Moreover, Herschel observations with the HIFI instrument (500 GHz - 2000 GHz) should allow obtaining a signal-to-noise ratio with a comparable spectral resolution in reasonable times. Such a high signal-to-noise ratio would enable us to better resolve the line wing shape in order to discriminate between both origins. Moreover, a temporal variability of the line could be brought to light. Such a variability should not be expected with an IDP origin. Indeed, Moses et al. (2000a) suggested that the production of the IDP is dominated by short-period comets. Selsis et al. (2004) showed that 48 short-period (~5-10 year periods) comets approach Jupiter's orbit at less than the Roche lobe radius of the planet. So, the IDP flux on Jupiter should be steady. Finally, using HIFI at the highest frequencies would result in a sufficient spatial resolution to carry out maps of Jupiter at water vapor frequencies. A latitudinal inhomogeneous distribution of water, with an increase of its amount in the southern hemisphere would be a strong signature of a SL9 impact origin and could provide information on the horizontal diffusion at the submillibar level.

References

[1] Berge, G. L., Gulkis, S., 1976, In "Jupiter, studies of the interior, atmosphere, magnetosphere and satellites", ed. T. Gehrels, 621-692

[2] Bergin, E. A., Lellouch, E., Harwit, M., Gurwell, M. A., Melnick, G. J., Ashby, M. L. N., Chin, G., Erickson, N. R., Goldsmith, P. F., Howe, J. E., Kleiner, S. C., Koch, D. G., Neufeld, D. A., Patten, B. M., Plume, R.,

Schneider, R., Snell, R. L., Stauffer, J. R., Tolls, V., Wang, Z., Winnewisser, G., Zhang, Y. F., 2000, The Astrophysical Journal, 539, L147-L150

[3] Bézard, B., Griffith, C. A., Kelly, D. M., Lacy, J. H., Greathouse, T., Orton, G., 1997, Icarus, 125, 94-120

[4] Borysow, J., Trafton, L., Frommhold, L., Birnbaum, G., 1985, The Astrophysical Journal, 296, 644-654

[5] Borysow, A., Frommhold, L., 1986, The Astrophysical Journal, 304, 849-865

[6] Borysow, J., Frommhold, L., Birnbaum, G., 1988, The Astrophysical Journal, 326, 509-515

[32] Brown, L. R., Peterson, D. B., 1994, Journal of Molecular Spectroscopy, 168, 593-606

[8] Dobrijevic, M., Parisot, J.-P., 1998, Planetary and Space Science, 46, 491-505

[9] Dobrijevic, M., Ollivier, J.-L., Billebaud, F., Parisot, J.-P., 2003, Astronomy and Astrophysics, 398, 335-344

[10] Dutta, J. M., Jones, C. R., Goyette, T. M., De Lucia, F. C., 1993 Icarus, 102, 232-239

[11] Feuchtgruber, H., Lellouch, E., de Graauw, T., Bézard, B., Encrenaz, T., Griffin, M., 1997, Nature, 389, 159-162

[12] Feuchtgruber, H., Lellouch, E., Encrenaz, T., Bézard, B., Coustenis, A., Drossart, P., Salama, A., de Graauw, T., Davis, G. R., 1999, The Universe as Seen by ISO, Eds., P. Cox & M.F. Kessler, ESA-SP, 427, 133

[13] Fouchet, T., Lellouch, E., Bézard, B., Feuchtgruber, H., Drossart, P., Encrenaz, T., 2000a, Astronomy and Astrophysics, 355, L13-L17

[14] Fouchet, T., Lellouch, E., Bézard, B., Encrenaz, T., Drossart, P., Feucht-

gruber, H., de Graauw, T., 2000b, Icarus, 143, 223-243

[15] Gladstone, G.R., Allen, M., Yung, Y. L., 1996, Icarus, 119, 1-52

[16] Hébrard, E., Dobrijevic, M., Bénilan, Y., Raulin, F., 2007, Planetary and Space Science, 55, 1470-1489

[17] Lellouch, E., Paubert, G., Moreno, R., Festou, M. C., Bézard, B., Bockelée-Morvan, D., Colom, P., Crovisier, J., Encrenaz, T., Gautier, D., Marten, A., Despois, D., Strobel, D. F., Sievers, A., 1995, Nature, 373, 592-595

[18] Lellouch, E., Bézard, B., Moreno, R., Bockelée-Morvan, D., Colom, P., Crovisier, J., Festou, M., Gautier, D., Marten, A., Paubert, G., 1997, Planetary and Space Science, 45, 1203-1212

[19] Lellouch, E., 1999, The Universe as Seen by ISO, Eds., P. Cox & M. F. Kessler, ESA-SP, 427, 125

[20] Lellouch, E., Bézard, B., Moses, J. I., Davis, G. R., Drossart, P., Feuchtgruber, H., Bergin, E. A., Moreno, R., Encrenaz, T., 2002, Icarus, 159, 112-131

[21] Levy, A, Lacome, N., Tarrago, G., 1993, Journal of Molecular Spectroscopy, 157, 172-181

[22] Levy, A, Lacome, N., Tarrago, G., 1994, Journal of Molecular Spectroscopy, 166, 20-31

[23] Moreno, R., 1998, PhD Thesis, Université Paris VI

[24] Moreno, R., Marten, A., Biraud, Y., Bézard, B., Lellouch, E., Paubert, G., Wild, W., 2001, Planetary and Space Science, 49, 473-486

[25] Moreno, R., Marten, A., Matthews, H. E., Biraud, Y., 2003, Planetary and Space Science, 51, 591-611

[26] Moses, J. I., Bézard, B., Lellouch, E., Gladstone, G. R., Feuchtgruber,

H., Allen, M., 2000a, Icarus, 143, 244-298

[27] Moses, J. I., Lellouch, E., Bézard, B., Gladstone, G. R., Feuchtgruber, H., Allen, M., 2000b, Icarus, 145, 166-202

[28] Moses, J. I., Fouchet, T., Bézard, B., Gladstone, G. R., Lellouch, E., Feuchtgruber, H., 2005, Journal of Geophysical Research, 110, E08001

[29] Olberg, M., Frisk, U., Lecacheux, A., Olofsson, A. O., Baron, P., Bergman, P., Florin, G., Hjalmarson, Å, Larsson, B., Murtagh, D., Olofsson, G., Pagani, L., Sandqvist, Aa., Teyssier, D., Torchinsky, S. A., Volk, K., 2003, Astronomy and Astrophysics, 402, L35-L38

[30] Ollivier, J.-L., Dobrijevic, M., & Parisot, J.-P., 2000, Planetary and Space Science, 48, 699

[31] Pickett, H. M., Poynter, R. L., Cohen, E. A., Delitsky, M. L., Pearson, J. C., Muller, H. S. P., 1998, Journal of Quantitative Spectroscopy and Radiative Transfer, 60, 883

[32] Selsis, F., Brillet, J., Rapaport, M., 2004, Astronomy and Astrophysics, 416, 783-789

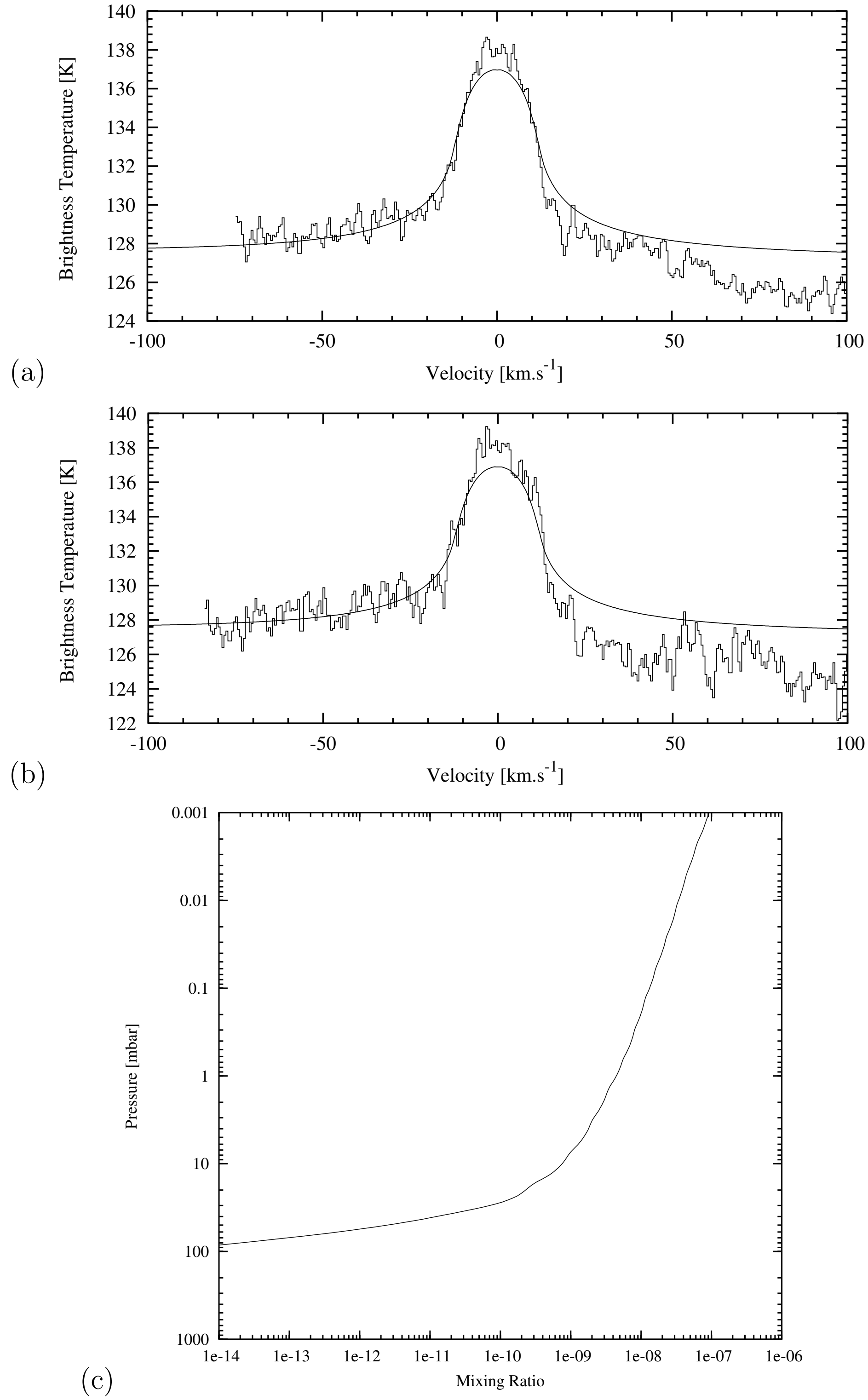

Fig. 7. Brightness temperature spectra as observed by SWAS (a) in 1999 and (b) in 2001. Both spectrum continuum have been rescaled so as to obtain a better fit of the line wings with an IDP model. (c): water mixing ratio vertical profile as a function of pressure resulting from the observed flux of $\Phi_{H_2O}^{IDP}$=3.7×10^6 cm^{-2}.s^{-1}.

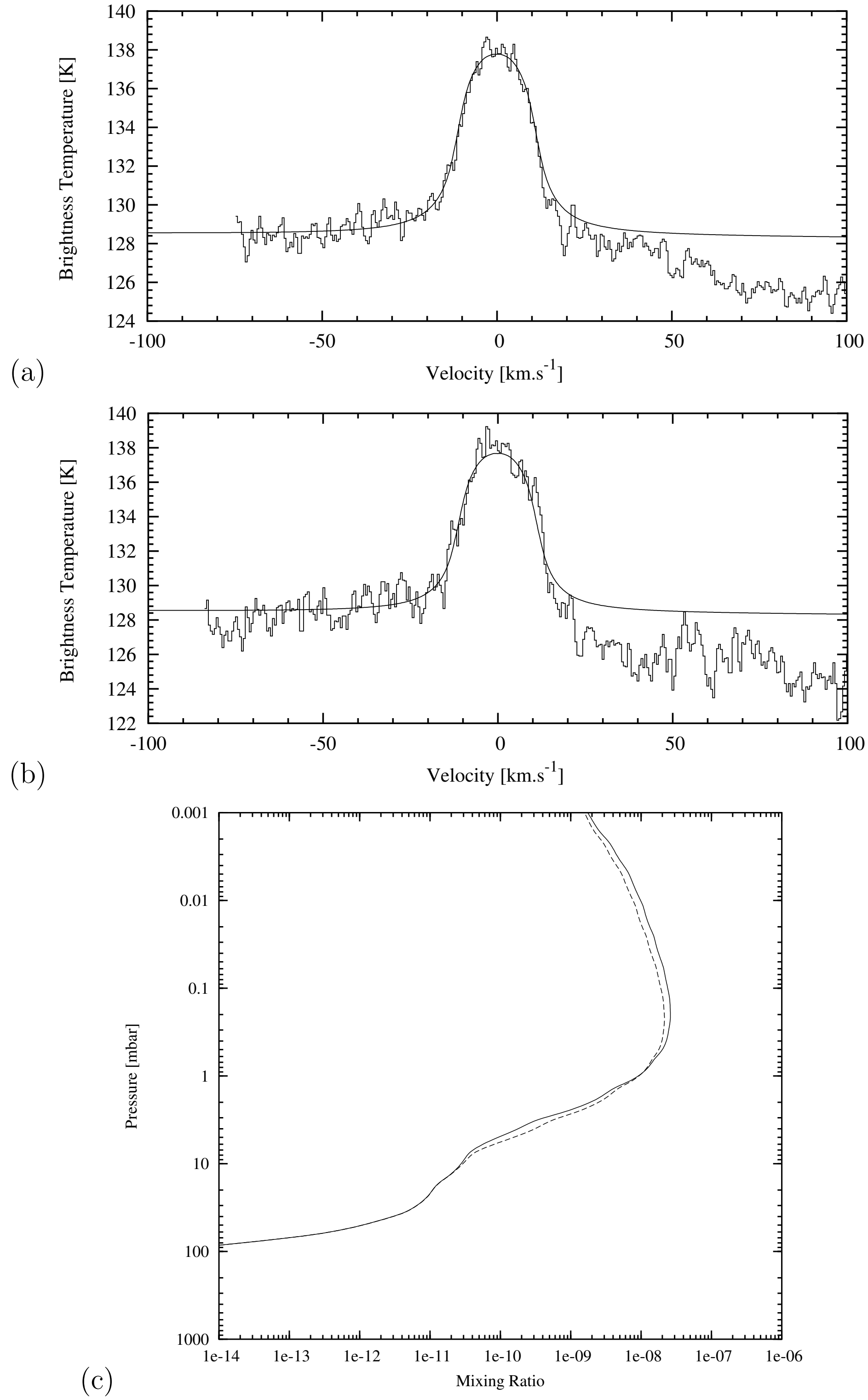

Fig. 8. SL9 model results compared to the (a) SWAS 1999 and (b) SWAS 2001 observed spectra, when fixing q_0=6.0×10^{-8}. The derived initial deposition pressure level p_0 is 0.45 mbar. (c): corresponding water mixing ratio vertical profiles at the time of the observations (solid line for 1999 and long-dashed lines for 2001).

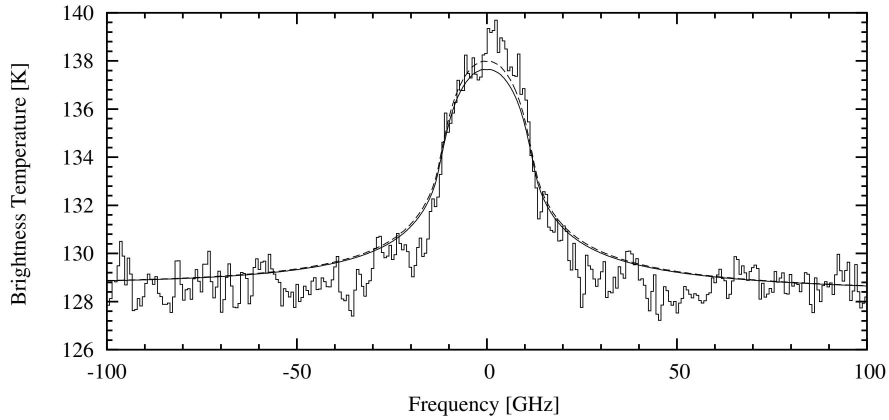

Fig. 9. Odin 2002 data modeled with IDP models. The solid line corresponds to a flux of $\Phi^{IDP}_{H_2O}$=3.4×10^6 cm^{-2}.s^{-1} (χ^2 minimum value). The long-dashed lines correspond to the overall (SWAS and Odin data) best-fit model ($\Phi^{IDP}_{H_2O}$=3.6×10^6 cm^{-2}.s^{-1}).

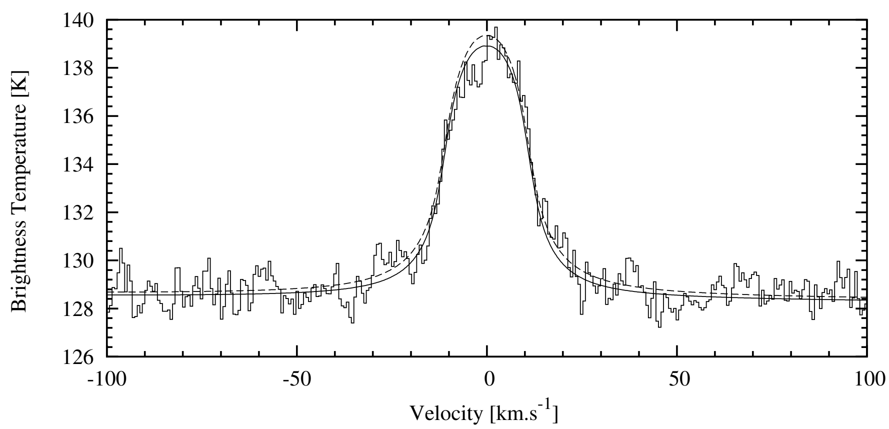

Fig. 10. Odin 2002 data modeled with SL9 models. When p_0 is fixed to 0.2 mbar, the derived q_0 value is 2.0×10^{-7} (solid line) whereas when fixing q_0 to 6.0×10^{-8}, the derived p_0 pressure level is 0.54 mbar (long-dashed lines).

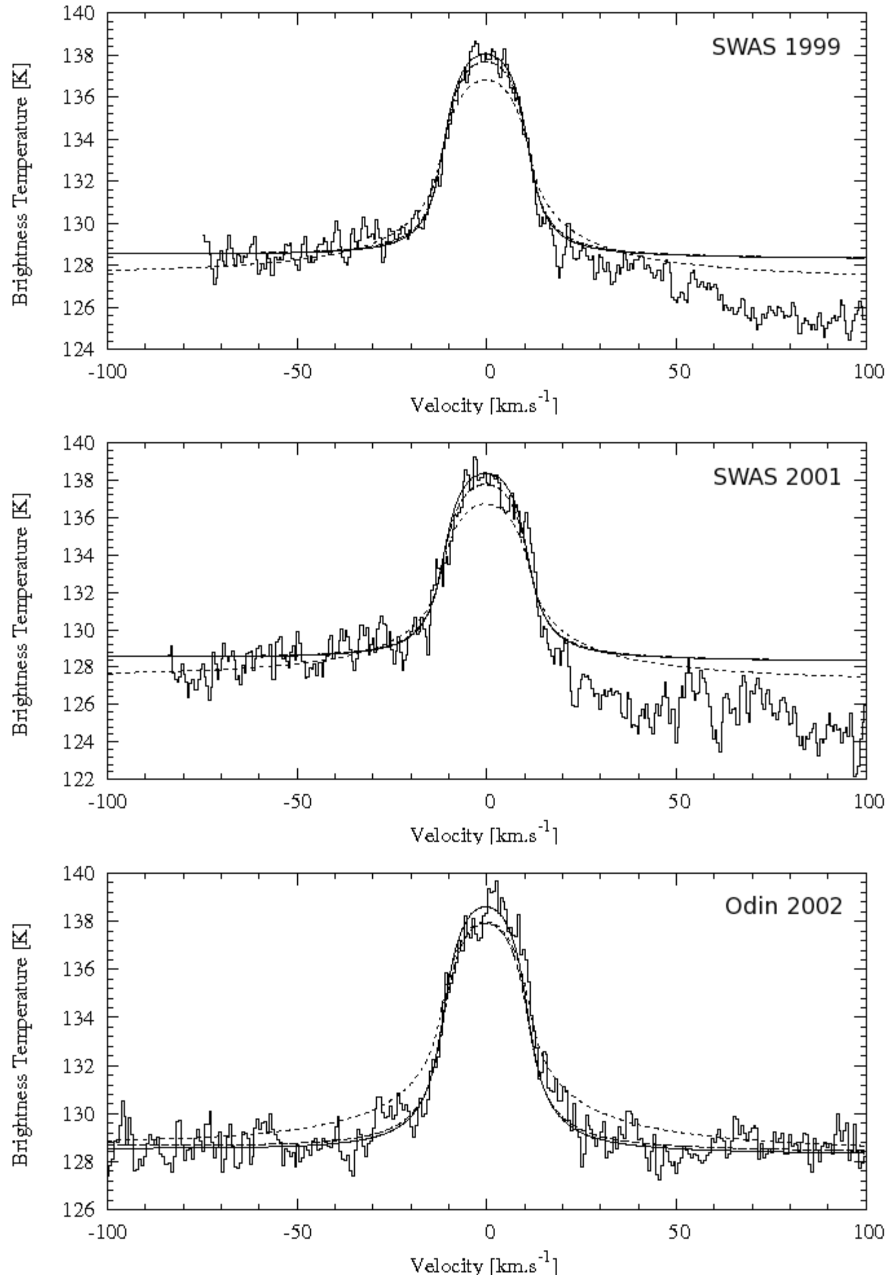

Fig. 11. Overall best-fit models for the SWAS 1999 and 2001 and Odin 2002 observations. Solid lines: SL9 model with p_0=0.2 mbar (fixed) and q_0= 1.9×10^{-7}; long–dashed lines: SL9 model with p_0=0.45 mbar and q_0=6×10^{-8} (fixed); short-dashed lines: IDP model with a steady infall flux of water $\Phi^{IDP}_{H_2O}$=3.6×10^{6} cm^{-2}.s^{-1}. The overall best-fit parameter have been obtained from Table 2 and by taking the signal-to-noise ratio of each observation into account. Doing this way, the SWAS 1999 observations have a lower impact on the results than the SWAS 2001 and Odin 2002 observations.

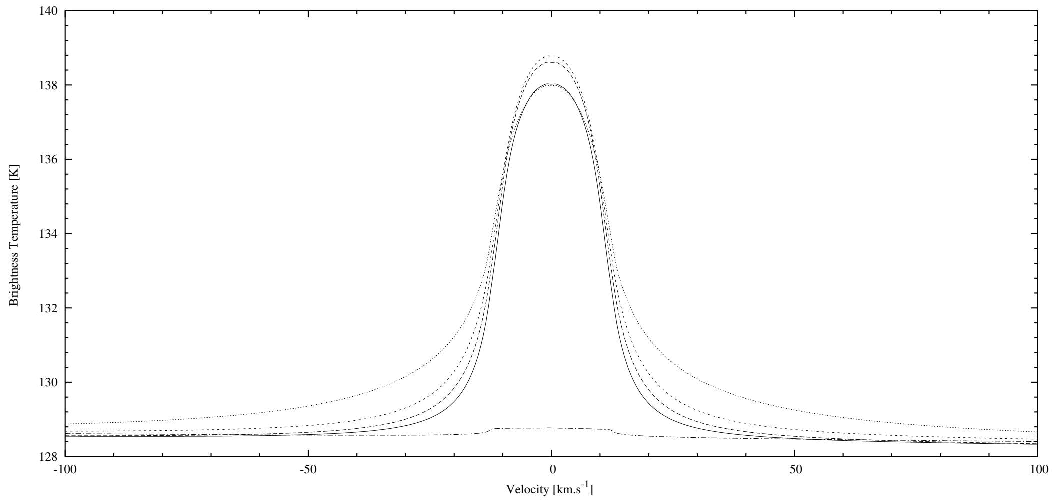

Fig. 12. Evolution of the line shape with time, in the case of a SL9 origin. Vertical distribution of water has been computed with our photochemical model at various dates. Parameters p_0 and q_0 have been set to 0.2 mbar and 1.9×10^{-7} respectively. The spectrum is plotted at the time of SWAS 1999 observations (solid line), Odin 2002 observations (long-dashed lines), in 2007 as observed with the Odin telescope (short-dashed lines). Once all the water deposited by SL9 will be removed by photochemistry, transport and condensation, the remaining water will only be due to the low IDP flux ($\Phi^{\rm IDP}_{\rm H_2O}$=$4 \times 10^4$cm^{-2}.s^{-1}). The dashed-dotted lines represent the line due to this flux, as it would be observed by Odin. The line resulting from an IDP model ($\Phi^{\rm IDP}_{\rm H_2O}$=$3.6\times10^6$ cm^{-2}.s^{-1}) is plotted for comparison in dotted lines.